

8-10-2015

# Geometric Element Test Targets for Visual Inference of a Printer's Dimension Limitations

Shu Chang

Heng Li

Nathan Ostrout

Monika Jhuria

Follow this and additional works at: <https://scholarworks.rit.edu/other>

---

## Recommended Citation

Chang, Shu; Li, Heng; Ostrout, Nathan; and Jhuria, Monika, "Geometric Element Test Targets for Visual Inference of a Printer's Dimension Limitations" (2015). Accessed from <https://scholarworks.rit.edu/other/843>

This Conference Paper is brought to you for free and open access by the Faculty & Staff Scholarship at RIT Scholar Works. It has been accepted for inclusion in Presentations and other scholarship by an authorized administrator of RIT Scholar Works. For more information, please contact [ritscholarworks@rit.edu](mailto:ritscholarworks@rit.edu).

# GEOMETRIC ELEMENT TEST TARGETS FOR VISUAL INFERENCE OF A PRINTER'S DIMENSION LIMITATIONS

S. Chang<sup>1,2,\*</sup>, H. Li<sup>1</sup>, N. Ostrout<sup>1</sup>, M. Jhuria<sup>3</sup>, S.A. Mottal<sup>1</sup>, and F. Sigg<sup>1</sup>

<sup>1</sup>*College of Imaging Arts and Sciences, <sup>2</sup>College of Science, and <sup>3</sup>Kate Gleason College of Engineering  
Rochester Institute of Technology, 69 Lomb Memorial Drive  
Rochester, Rochester, NY, 14623, USA.*

*\*Corresponding Author  
E-mail: shu.chang@rit.edu*

## **Abstract**

As technologies advance in the field of additive manufacturing (AM), it increases the demand in using test targets to quantitatively appraise the performance of AM processes and parts. This study presents a unique concept to address the dimensional and geometric viability of three-dimensional (3D) printers with test targets that are unique and complementary to those currently available. We have named these distinct designed artifacts as Geometric Element Test Targets (GETTs). The concept for the targets is to rely on positioning and spatial frequency of geometric shapes to induce failures that are indicative of the system's dimensional limitations. A distinguishing characteristic is that the dimensional failures can be inspected visually. Systematic evaluations of the limitations can be further conducted through contact or non-contact measurements. The initial GETTs include three suites of test targets: line, angular and circular suites. We will illustrate this concept with samples produced with fused deposition modeling printers. The potential applications of GETTs include standardization, reference targets, in-line system control, and more.

## **1. Introduction**

As technologies proliferate in additive manufacturing (AM), the competence to quantify the ability of fabrication processes to produce consistent and defect-free parts with intended dimensions has become an important and central requirement in the AM technology advancement. The AM community has recognized that there is a high demand for measurement science in order to achieve predictable and repeatable operations and quality products [1].

Numerous test artifacts have been developed and used to find the accuracy printed parts or to benchmark the performance of AM machines and have been well summarized in recent publications by S. Moylan et. al. [2 and references therein], [3 and references therein] and L. Yang and M.A. Anam [4 and references therein]. These standard test artifacts focus on the dimensional and geometric accuracy of intentionally designed and coordination-wise positioned [2]-[4]. The test artifacts include basic geometric shapes such as cylinders, cubes, etc. (will refer to as

fundamentals) as well as super-positioned geometric shapes such as combined or free forms (will refer to as composites). The artifacts are strategically positioned with the intent to expose changes and faults in dimensional and geometric attributes [2]-[4]. The shapes are either solitary units or the repetition of same/different sizes.

The measurement tools can be gauges, calipers, micrometers, coordinate measuring machine (CMM), profilometer (contact or non-contact), optical microscopes, etc. The methodology used are measurements of coordination points and then least square fitted to reference CAD models [2]-[4]. The measurements focus on both dimensional accuracies and geometric accuracies, which Yang and M.A. Anam [4] have summarized into six attributes: straightness, parallelism, perpendicularity, roundness, concentricity, and true positions (for pin and for z-plane).

These test artifacts have been used to measure part accuracies as well as benchmarking different AM technologies. There has been a call for complementary targets that “in order to reveal more information about the process quality, the features of the standard test part for process development should be designed in such a way that slight deviations from optimal process parameters would result in significant defects” [4].

The intention of this research is to address this demand and to present Rochester Institute of Technology’s Geometric Element Test Targets (GETTs). GETTs assess the dimensional and geometric viability of three-dimensional printers and processes with a unique test target concept transpired from two-dimensional (2D) graphic printing. These GETTs focus on the 3D printers’ dimensional viability (the dimension which can no longer be produced because of the system uncertainty) and the geometric viability (the geometric shape which fails to maintain the original or the designed form and orientation). GETTs also provides the possibility to determine the process capability visually in addition to measurements through metrological instruments. The following sections will present a few selected concepts of 2D graphic targets, the translation of the 2D targets into GETTs, and our initial validation of the concept on GETTs.

## **2. Test Artifacts Practiced in Two-Dimensional Printing**

In 2D graphic printing, it is common to use test targets to stress a printing system’s attributes and elicit responses from different subsystems to assess the process’ performance [5]. Similar to AM test artifacts, the 2D test targets such as those produced by RIT are consist of fundamental (lines, dots, grey level, etc.) and composite (pictorial) elements. The fundamental targets are typically used for visual inspection or quantitative measurements of production/reproduction dimensional and geometrical viability while the composite images are for assessing human psycho-physiological responses through ranking [6].

Many fundamental 2D graphic targets rely on inducing failures in the production of intended amplitudes of repetitive patterns at high spatial frequencies. The decrease in pattern sizes is to locate where the pattern will be distorted during the printing process. Some of the failures will have distinguished characteristics that can be identify visually (or through an eye loop) while others will require instrumental and statistical assessments. 2D graphical targets are utilized to measure systematically these responses additionally in order to establish a transfer function between the digital representations and their corresponding print quality. An example of a system distortion is the laser beam size or charge spreading on the surface of a photoconductor in electrophotographic printers where the effect of addressability size is determined through the use

of targets, and later used to predict output image quality. The elemental targets typically consist text, curved and high spatial frequency lines, and halftones at different gray levels as exemplified in [5], [6], [7], [8], [9].

In this paper we will introduce three standard targets which are widely practiced in graphic and document reproductions, namely, a checkerboard, a ray, and a concentric circle pattern. These three patterns have characteristics that are deemed applicable to 3D printing and will be our initial focus for consideration on potential 3D targets.

Figure 1 shows a checkerboard target which is a snap-shot from the corresponding region in the Synthetic Targets from RIT's test targets publications [7]. The checkerboard pattern is used for assessing printer's dimensional resolution and dot gains. Figure 1 also contains a sequence of checkerboard patterns with increasing checker size, labelled as "1 dot by 1 dot" and so forth. These numerical figures represent the number of addressable dots in each checker square area (either on or off for black or white respectively). The checkerboard in Figure 1 was designed for a printer with an addressability of 600 dots-per-inch (dpi); that means "1 dot by 1 dot" checker square has an area of  $42.3 \mu\text{m} \times 42.3 \mu\text{m}$ . When used for dimensional examination, a printer's resolution will be the "x dot by x dot" block where the pattern is clearly discernable visually or through eye loops. The checkerboard pattern can also be measured using a scanner or a microscope. The dot gains will be reflected in the over or under filling of the checker area through the instrumentation measurement.

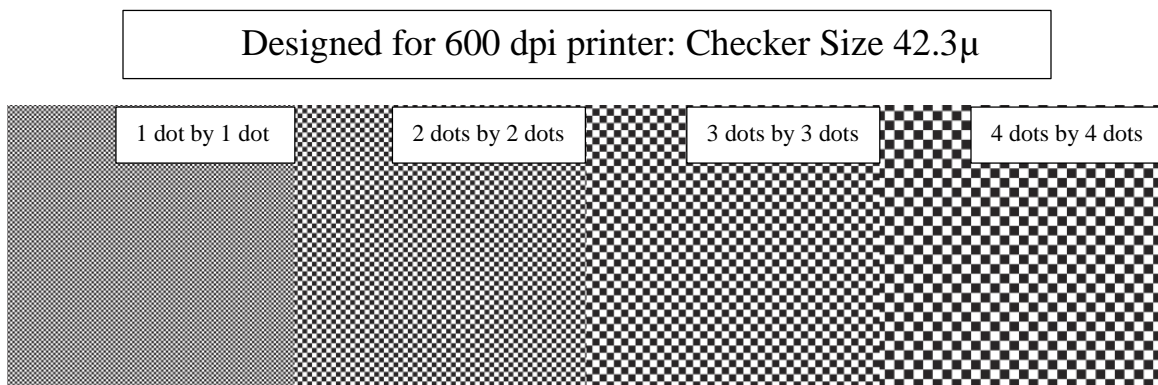


Figure.1. Example of RIT's checker board resolution target that identifies the dot-by-dot dimension that a printer can produce and the amount of over or under filling of checker areas for process dot-gain or dot-loss.

Depicted in Figure 2 are ray charts which are predominately utilized in resolving orientation-dependent dimensional feasibility. Figure 2 contains two simulated ray targets as contrast to illustrate the impact of the imaging spot aspect ratio (such as a laser spot) on the print quality [10]. The left ray target is simulated with a square spot and the right with an elliptical spots oriented at  $45^\circ$  (with zero being the horizontal line). The spots are indicated at the lower left corner of each ray target respectively. The square spots on the left have resulted in a uniform distribution of lines shown in the left target. The directional printing spots, or the elliptical spots, give rise to an anisotropic distribution of ray densities. The directional density distribution is revealed in the right ray target as emphasized by a darker banding oriented at  $135^\circ$  and perpendicular to the original spot orientation.

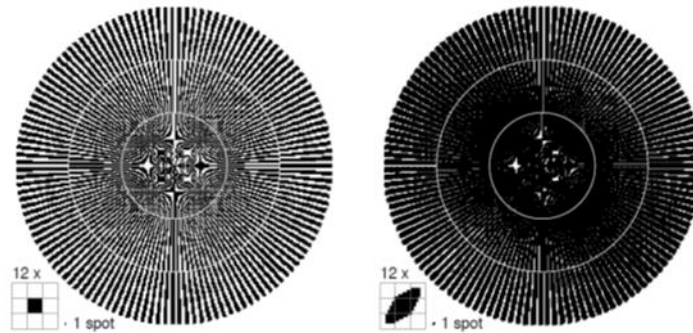


Figure.2. Specifically designed features such as the ray lines draw out system responses, in this case the directional effect, from the printing processes.

Figure 3 is a concentric circle target also known as the contrast-resolution test target [10]. The main features in Figure 3 are sets of concentric rings, with equally black and white spacing. Figure 3 presents the concentric rings at decreasing contrast (defined as the ratio of reflectance of two areas in an image) horizontally and increasing spacing frequency vertically. This circular target probes the capability of a printing system to reproduce fine detail of various orientations, frequencies, contrast and tonal values (similar to grey levels). Similar to the checkerboard resolution target, system effects can be reflected in the target, as demonstrated by the impact from difference halftone screens in the work of F. Sigg and D. Romano [8].

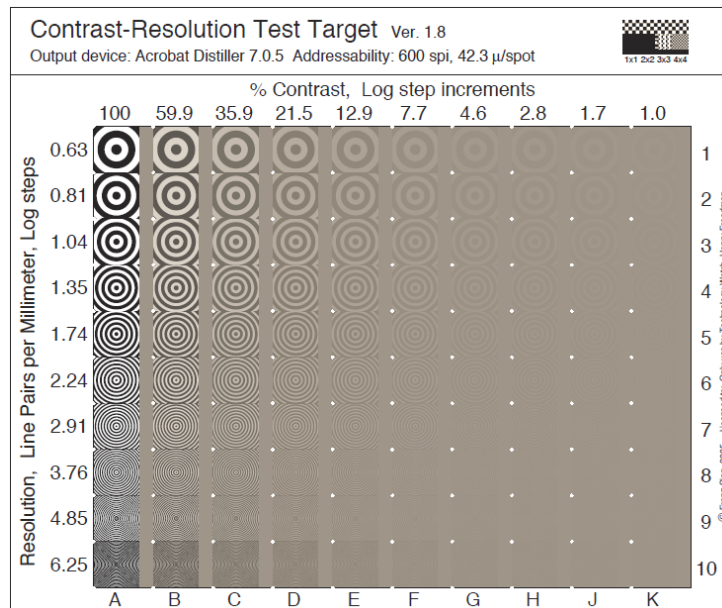


Figure.3. Contrast-resolution test target [11] that identifies the cut-offs for both tonal contrast and spatial resolution for printers.

The patterns illustrated in Figures 1-3 are typically of what printing professionals rely on to calibrate and optimize print systems as well as to identify process failures. Quantifiable metrics for fundamental print patterns have been developed with standards to be used with microscopes and scanners. Standards are also established for composite or pictorial images to be qualitatively assessed with rankings. A point to notice, the fundamental patterns are what have been used for in-process quality assurance, process controls, and printer's models [11].

### **3. Translation of Test Targets from 2D to 3D**

The objective of the translation of 2D test target into 3D aims at developing a simplified inspection tool and working standard to determine a printer's capability. The intent is to complement the existing test artifacts which provide quantitative assessments of the produced geometric shapes and parts [2]-[4]. The research has a long term goal at develop geometric element test targets to assess system responses of AM processes and to establish functional relationships between the responses and process parameters. By exploiting and measuring systematic limitations, GETTs has the potential for in-line assessments and process controls.

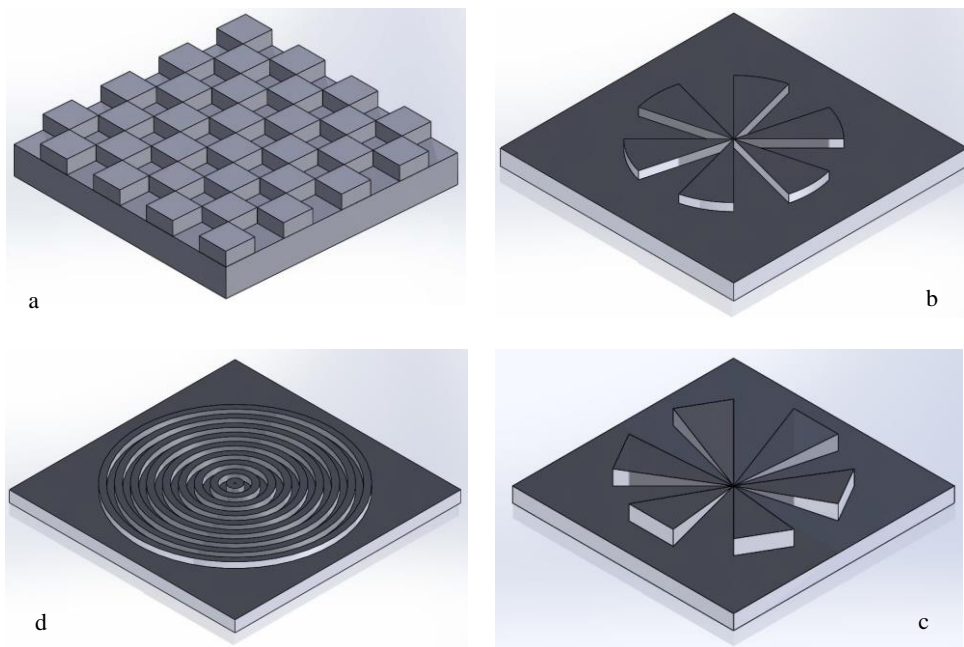


Figure.4. Perspective view of checkerboard (a), flat ray (b), slanted ray (c), and concentric circle (d) GETTs respectively.

We have constructed three suites of GETTs, line, angular, and circular suites in the likeness of their 2D counterparts. Our focus of this work is on the GETTs presented in Figure 4. Figure 4 shows few examples of GETTs (presented counter-clockwise from top-left, a checkerboard (a), a flat ray (b), a slanted ray (c), and a concentric circle (d)). As illustrated in Figure 4, the contrast attribute in 2D graphics is replaced here by the height for both the checkerboard and concentric circle GETTs. The ray target, however, has been translated into flat and slanted rays. The slanted ray varies in z-dimension with a convergence to zero at the center of the ray.

The design of GETTs follow the following guidelines:

- The fundamental units of GETTs are simple geometric elements, such as cubes, triangular wedges, cylinders, etc.
- The placements of elements are in reference to the process-related orientations.
- GETTs contain repetitive elements with diminishing sizes and amplitudes (heights).
- The dimensional range for GETTs design is based on the minimal addressability of the printing device under examination. When the accurate addressability is not known, standard measurement such as a metric or an English system is used considering the smallest element size to be less than the addressability but of the same order if possible.
- The dimensional changes might be continuous or discrete.
- The elements can be positioned in isolation, intercepted, or integrated with either the same or different elements.
- Elements can be raised or recessed with respect to a reference plane.
- For integrated targets such as ray chart, create convergence.

Expanding from 2D graphic target design has been attempted recently. B.H. Jerad et. al. have explored the conversion of the ray chart (also known as Siemens star) into a 3D artifact [12]. His adaptation is a star of a raised center and has diminishing star arms pointing outwards. The star was designed for quantitative measurement. Here the ray GETTs have raised edge with dimensional convergence to zero height at the center of the ray. This ray has the potential for both visual inspections and quantitative metrological instrumentations.

In the same publication, B.H. Jerad et. al. [12] also create a “Manhattan” test artifact for examining dimensional accuracy throughout the 3D space. The “Manhattan” test artifact consist separated squares of the same areas at different heights for measurement at various positions in space, The GETTs checkerboard have the same height for each checkerboard unit. The checkerboard GETTs is to reveal a printer or a print process’ planar resolution.

The existing artifacts also incorporate the technique in which a series of structures are decreasing in size and repeating geometric shapes [2]-[4], [13]. The repetitions are directed at covering measurement accuracy and precision for a range of dimensions [2]-[4], [13] and do not appear to be for graphic test target applications.

#### **4. Validation of GETTs**

We have two Fused Deposition Modeling (FDM) engines, a MakerBot® Replicator 2X and a LulzBot TAZ 3 at our disposal. The FDM process drives a thermoplastic wire to the heater and melts the thermoplastic to deliver the molten material through a nozzle [14]. The process thus deposit a thread of thermoplastic material to builds the part line by line and then layer upon layer on a base platform. Although both of low resolutions and one technology, the two machines offer a comparison and contrast for the two systems.

The designs of the GETTs were prepared by using SolidWorks 3D modeling software. The design files are in STereoLithography (STL) format. We used Acrylonitrile Butadiene Styrene (ABS) in the validation experiment.

For this study, both machines are set at default values with the assumption that these have been optimized by the original engine manufacturers (OEM). In this case both the printers have extrusion temperature set at 230 °C. The bed temperatures, however, are at difference values of 110 °C and 85 °C for MakerBot and LulzBot respectively. We selected the infill density to be 10% for both the printers. As per OEMs' specifications, the MakerBot has a nozzle opening of 0.4 mm and LulzBot of 0.35 mm.

Photographs were taken with a Canon EOS 5D Mark III camera. SOFV-1 light booth made by Graphic Technology provided the lighting for the photographs. Microscope images were captured using VHX-2000E series microscope made by Keyence® Inc at 20X magnification. The photographs are mostly used to demonstrate the feasibility of visual dimensional assessment. The images are captured by the microscope when better observation of specific characteristics are called for. The microscope has been set to minimal magnification to simulate the situation of inspection with eye-loops.

The following Figures (5-9) concentrate on the concept of graphical patterns for distinguish system attributes and features. Figure 5 depicts an example of the checkerboard pattern used to determine and compare the ability of two FDM printers to resolve square features in the horizontal plane. Exhibited in the left side of Figure 5 (Figure 5A) are photographs of four GETT™ checkerboard samples fabricated with the MakerBot. Positioned clockwise at decreasing checkerboard length and width, starting with the top-left photograph is the target that has checkers of 10 mm in length and width and 1 mm in height. The three checkerboards in Figure 5 have decreased dimensions of checker's length and width to 5 mm, 2.5 mm, and 1.25 mm respectively, all are at 1 mm height. Exhibited in the right side of Figure 5 (Figure 5B) are the same GETTs produced with the LulzBot and presented in the same fashion.

For MakerBot GETTs, the square shapes are well resolved in the 10 mm, 5 mm and 2.5 mm print samples, although there is some rounding at the corners of the 2.5 mm checkers. For the 1.25 mm checkerboard, however, the corners of the squares diminish and appear as circular protrusions instead of the angular squares. In comparison, the disappearance of corners come at 2.5 mm for the LulzBot GETTs. For the LulzBot samples, the checkerboard shape cannot be reproduced and lost its periodicity at 1.25 mm.

According to manufacturer's specifications, the MakerBot has a nozzle opening of 0.4 mm and the LulzBot has of 0.35 mm. Figure 5 indicates that for both the machines resolutions are far worse than the sizes of the nozzle openings or their addressability. Figure 5 shows that the MakerBot appears to have a superior square-resolving ability than that of LulzBot.

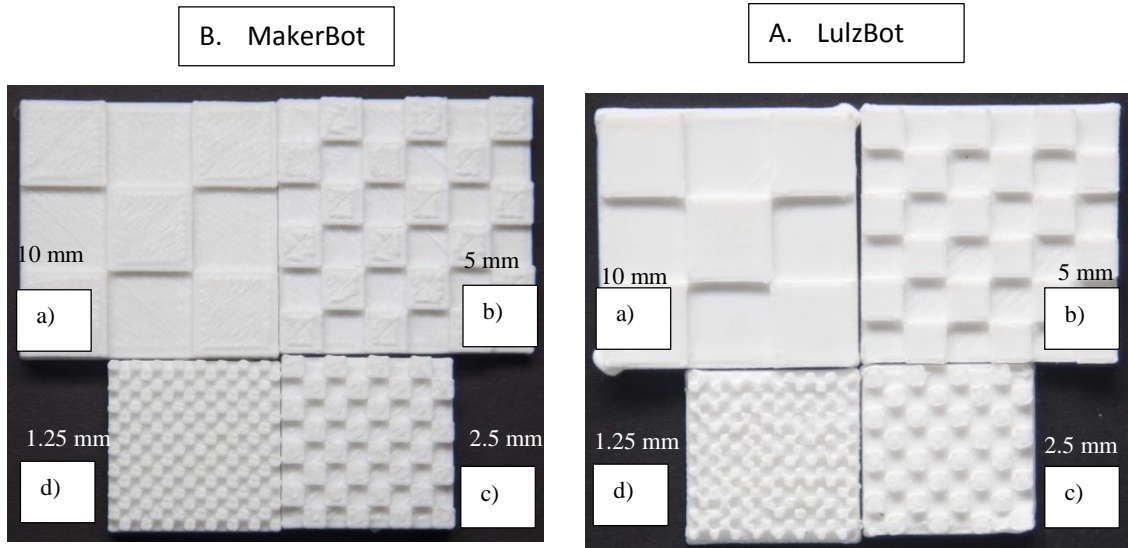


Figure.5. A sequence of decreasing sizes of checkerboard patterns shows resolution limitation difference of two FDM devices to produce squares. The device that produced the left group of GETTs, MakerBot, loses its ability at about 1.25 mm checker size. In contrast, the device that produced the right group of GETTs, LulzBot, fails at about 2.5 mm checker size.

A set of flat ray samples are depicted in Figure 6 to illustrate their role in revealing the limit of printable line widths. All pie-shapes in the five ray GETTs are designed to have a length of 10 mm and a height of 1 mm. The pies have equal widths for both protruding features and separations in-between in each chart with the first on the left with the largest and the last the smallest partitions. The five ray GETTs in Figure 6 consequently have increasing number of pies: 6, 9, 12, 15, and 18 and are displayed from left to right respectively. The targets here are printed with the MakerBot printer.

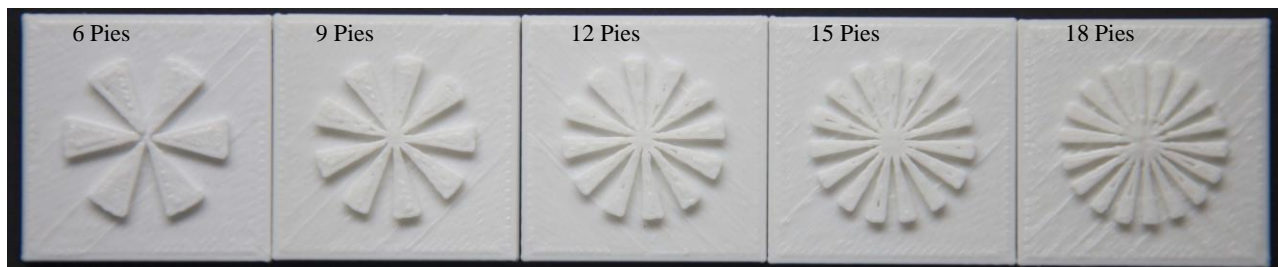


Figure.6. A sequence of increasing number of pies in ray GETTs. The resulted center rings mark the areas that the printer has failed to print. These areas can be used to calculate the resolvable line width.

The intent of the ray GETTs design is for the dimensions to converge to a singularity point at the center in this example. As this singularity is impossible to be produced by the printing system, a forbidden ring will emerge at the center of the ray. The size of the forbidden ring reflects the line width producible by the FDM system. As indicated in Figure 6, the size of the forbidden ring grows in the proportion to the increase in the number of pies in the ray. This is because when the pie width gets narrower, the position of dimensional failure moves outward. If one may estimate the diameters of the rings presented in Figure 6 (say using the 15 pie ray chart here to get an about 4 mm diameter) and estimate the pie widths at which the failure occurs, a roughly 0.4 mm width can be obtained. With the OEM specified nozzle opening of 0.4 mm, the deposition process appears to transform a  $\pi \times (0.4)^2 \text{ mm}^2$  circular area into a roughly rectangular area of 0.4 mm base and thereby an about 0.3 mm height. Since the thermoplastic material will flow upon contact with the substrate, we expect to observe gains in widths of lines and loss in heights of lines.

In complementary to the flat ray target, the slanted ray GETTs can be used to determine a FMD printer's z-direction effective addressability. Figure 7 shows two six-pie ray GETTs whose designed dimensions are 2 mm in height at the end of the wedge and converging to zero height in the center with the pie length being 10 mm. The images here are capture with Keyence® VHX-2000E series microscope by at a 20X magnification to better revealing the details at the center and the steps. As with the flat ray GETTs in Figure 6, both of them demonstrate the forbidden zones. In addition the photographs show steps on the incline plane due to the nature of the FDM technology.

Comparison of the two photographs reveals that for the same designed height MakerBot has generated 9 steps the printed sample while LulzBot only 6 steps. Measuring the resulting wedge heights indicate a reproduction of 2 mm with the MakerBot but only 1.6 mm with the LulzBot. Dividing the heights with their respective steps shows that MakerBot has a higher z-direction addressability of 0.22 mm/step than that of 0.26 mm/step from the LulzBot. In addition, only about half of the pies indicate distinguishable steps in the LulzBot target image. Furthermore, LulzBot target image has a larger failed area at the center than the MakerBot target image, also depicting the inferior of dimensional resolution of the LulzBot machine.

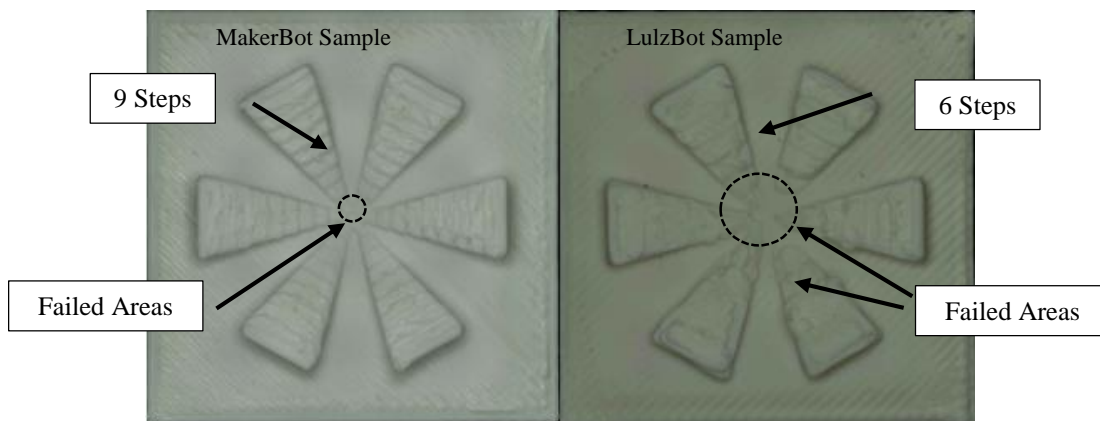


Figure.7. Convergent slanted ray GETTs divulges FDM printers' z-direction addressability through the number of steps on the slanted plane for a given height.

Depicted in Figure 8 are two concentric circle GETTs produced using the MakerBot. The two GETTs are designed to have 2 mm line protrusion heights but different spacing frequencies: 1 mm line width for GETT in Figure 8a and 0.5 mm line width for GETT in Figure 8b. A close inspection of the photographs reveals directional effects in Figure 8a, which shows distinct regions (as an example sections in Figure 8a separated by dashed lines) where the printed lines split while other regions the lines remain intact.

As the line width is reduced (Figure 8b), the printed lines seems to be at the printer’s resolution and no longer split. However, there is noticeable unevenness in the line separation while other regions maintaining the line spacing and width. As examples, two areas in Figure 8b are identified with arrows and marked as “Increased Gap” and “Decreased Gap”. In addition, a narrow section around 9 o’clock in Figure 8b exhibits a well-defined section which marks the start and end points of print process.

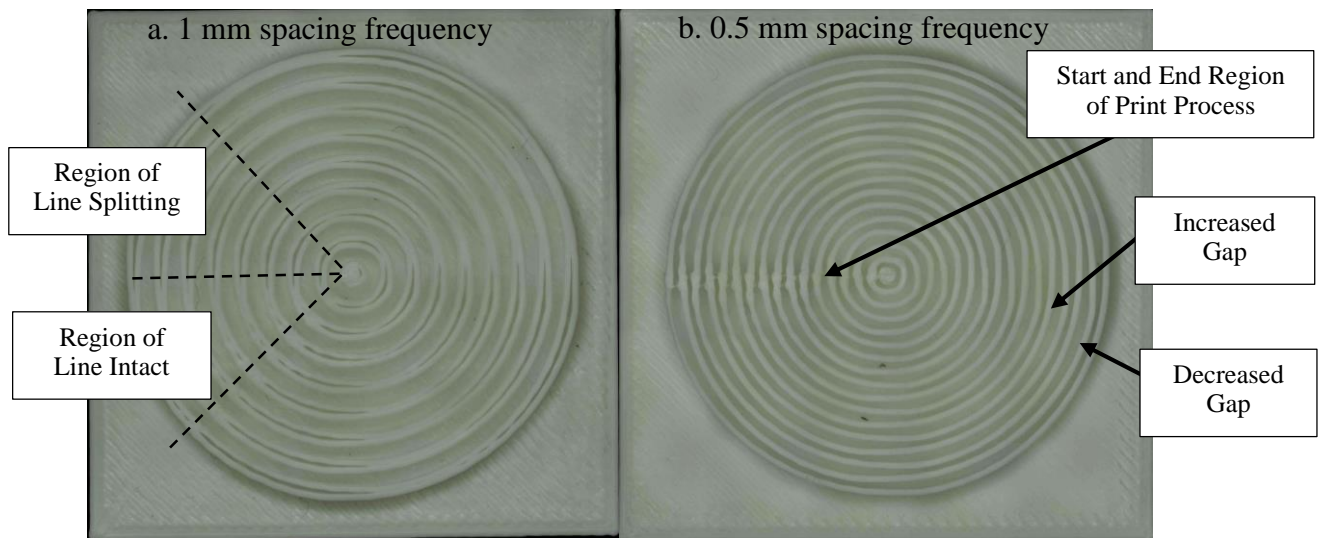


Figure.8. Concentric circle targets to illustrate defects of FDM printing: line splitting, deviations in print paths, and visible joining of start and end points.

We have assembled sequences of concentric circle targets similar to the 2D contrast-resolution target to present a “bird-eye” view of how variation in heights and widths of line impacts the printer’s ability to reproduce the 3D circular element. In Figure 9 we replace the “contrasts” to line heights and present the same line width GETTs with diminishing line height horizontally from left to the right of the constructed assembly. We place the same height GETTs at increasing spatial frequency vertically from top to bottom of the assembly. The concentric circle GETTs shown in Figure 9 are fabricated with the help of the MakerBot printer.

By comparing the targets horizontally, we do not observe much difference in the GETTs production with changing line height. This is expected since the nature of DFM material deposition is to draw lines, In contrast when comparing GETTs vertically, the change in line spatial frequency has introduced a number of faults as already discussed for Figure 8. In addition the vertical contrast reveals that when the spacing frequency is reduced to 0.25 mm, the concentric circle GETTs cannot be produced regardless of the line height.

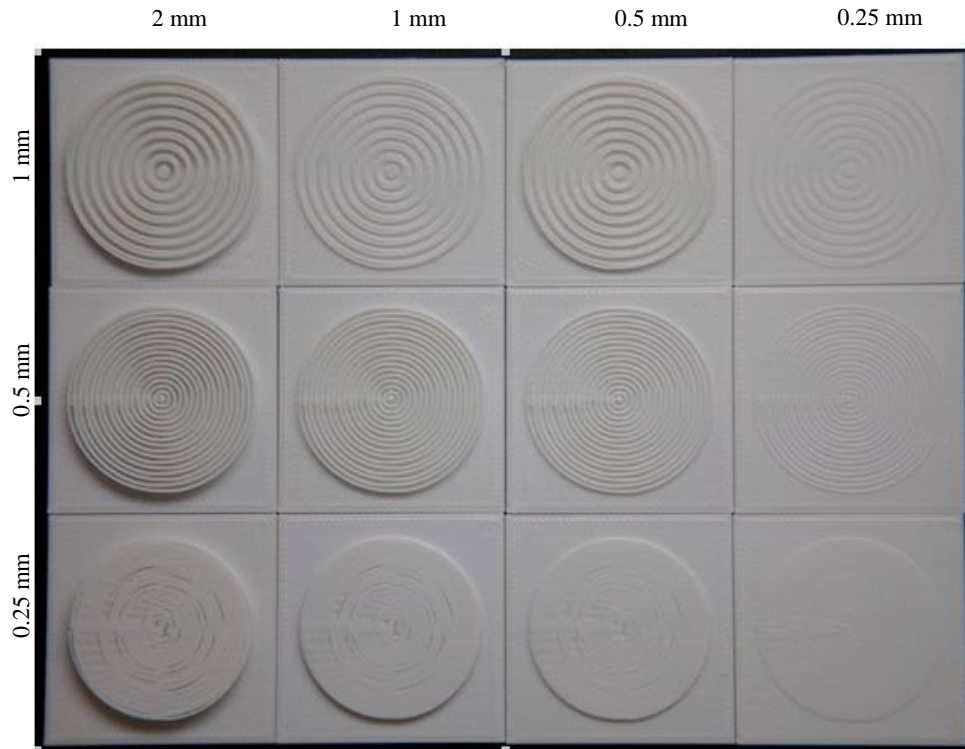


Figure.9. Height and frequency resolution concentric circle GETTs to detect dimensional failures and deviations.

## 5. Potential Usage

In 2D graphic and document production industry, targets are generally produced using high resolution printers and then used as references for both visual inspections and measurement standards for quality control. They are also widely used to calibrate printers on manufacturing consistencies within the same processes and to benchmark different processes. It is a common practice to have specific targets integrate into the printer's process controls and feedbacks. The targets are also employed widely in the interactions with customers for meeting their requirements and for providing proofs for the quality of the products. With research and exploration, GETTs has the potential to attain all these uses in the AM industry.

As for research and technology development, GETTs offer a method to examine and optimize system performance as functions of process critical parameters and material specifications. Determinations of functional responses will enable tradeoffs between objectives and attributes in the engine architecture designs. Furthermore, with the establishment of a printer's fundamental dimensional and geometric capability, there is a potential to predict and simulate build parts.

## **6. Conclusion**

This study presents a graphical concept to address the dimensional and geometric viability of 3D printers with test targets, named as GETTs that are complementary to those currently available. This study has validated that dimensional failures can be observed and estimated visually with systematic target designs. The GETTs examples from three suites of test targets (line, angular and circular) presented in this study have demonstrated the feasibility in detecting geometric and dimensional errors. With further validation with high addressability machines and more machine-specific target designs, GETTs have the potential as a simplified print quality inspection tool, a working standard, a target for in-line system control, and for studying the system or subsystem responses to process parameters.

The aims of this research are to develop geometric element test targets and measurement methodologies and to assess system responses of additive manufacturing (AM) processes. By exploiting and measuring systematic limitations, the project seeks to determine transfer functions between digital representations and printed parts as well as to explore opportunities for use of the GETTs in in-line assessments and process controls.

## **Acknowledgements**

This research is supported by the Melbert B. Cary Jr. endowment from the College of Imaging Arts and Science at Rochester Institute of Technology.

## **References**

- [1] NIST's Measurement Science for Additive Manufacturing Program [online]. Available at <http://www.nist.gov/el/isd/sbm/msam.cfm>.
- [2] Shawn Moylan<sup>1</sup>, John Slotwinski, April Cooke, Kevin Jurens, and M. Alkan Donmez, "An Additive Manufacturing Test Artifact," in Journal of Research of the National Institute of Standards and Technology, Volume 119, pp. 429-459, 2014.
- [3] S. Moylan, J. Slotwinski, A. Cooke, K. Jurens, and M. A. Donmez, "Proposal for a Standardized Test Artifact for Additive Manufacturing Machines and Processes", Proceedings of the Solid Freeform Fabrication Symposium, Austin, Texas, August 6-8, 2012.
- [4] Li Yang, Md Ashabul Anam, "An investigation of standard test part design for additive manufacturing," proceeding in Solid Freeform Fabrication Symposium, pp. 901-922, 2014.
- [5] Robert Chung, Fred Hsu, Michael Riordan, Franz Sigg, "Test Targets 8.0: A Collaborative effort exploring the use of scientific methods for color imaging and process control," 2008.
- [6] Eric K. Zeisea, D. René Rasmussenb, Yee S. Nga, Edul Dalalb, Ann McCarthyc, and Don Williamsd, "INCITS W1.1 development update: Appearance-based image quality standards for printers," Proceedings of Spie-the International Society for Optical Engineering, Vol. 6808, Jan 2008.

- [7] Robert Chung, Franz Sigg, Dimitrios Ploumidis, "Test Targets 6.0: A Collaborative effort exploring the use of scientific methods for color imaging and process control," RIT School of Print Media Publication, Nov. 2006.
- [8] F. Sigg and D. Romano, "How to Calibrate and Linearize an Imagesetter Using the Digital UGRA/FOGRA Wedge", Society for Imaging Science and Technology, Proceedings of the Fourth Technical Symposium on Prepress Proofing and Printing, Oct. 1995, pp. 88-92.
- [9] F. Sigg, "Ray\_Doc\_6", Rochester Institute of Technology, May, 2005.
- [10] Franz Sigg, "Testing for Resolution and Contrast," RIT School of Print Media Publication, Id TF\_12, version v2.2.
- [11] H. Mizes, "Empirically Based Printer Model of Halftone Structure", NIP & Digital Fabrication Conferences, Vol. 2004, No. 1, 2004, pp. 35-40.
- [12] Bradley H. Jared , Hy D. Tran , David Saiz , Christopher L. Boucher , and Joseph E. Dinardo, "Metrology for Additive Manufacturing Parts and Processes," Spring Topical Meeting, vol.57, 2014
- [13] D. Dimitrov, "Advances in three dimensional printing – state of the art and future perspectives," Rapid Prototyping Journal, Vol. 12 Iss 3 pp. 136 – 147, January 2006.
- [14] Chua, Leong, Lim C.S 2010," Rapid Prototyping: Principles and Application, 3rd Edition, World Scientific Publishing" Co. Pte. Ltd, 2010, 512p.